Available online at www.sciencedirect.com

ScienceDirect

Procedia Structural Integrity 13 (2018) 261–266

Structural Integrity Procedia

www.elsevier.com/locate/procedia

ECF22 - Loading and Environmental effects on Structural Integrity

Crack growth monitoring in corrosion-fatigue tests using back face strain measurement technique

Ali Mehmanparast[a]*, Pietro Albani[a], Victor Igwemezie[a]

[a]Offshore Renewable Energy Engineering Centre, Cranfield University, Cranfield, MK43 0AL, UK

Abstract

Corrosion-fatigue crack growth tests are known to be considerably time consuming, particularly due to low loading frequencies which often result in several months of testing. This study focuses on development of a material and load dependent numerical model which correlates back face strains with crack lengths for standard compact tension, C(T), specimen geometry. To validate numerical predictions, calibration fatigue crack growth tests were conducted in air on C(T) specimens made of S355 steel, which is widely employed in offshore wind industry. The results obtained from these tests at different load levels have been compared with those predicted from the numerical model. Characterization of isotropic-kinematic hardening behaviour for the material adopted was carried out using the data available in the literature. The numerical model presented in this work has proven to generate accurate estimates of crack length in corrosion-fatigue tests. This model can be used in future experimental test program on S355 steel without needing to obtain experimental correlations between crack length and back face strains from calibration tests performed in air.

Peer-review under responsibility of the ECF22 organizers.

Keywords: Crack growth monitoring; Fatigue.

1. Introduction

One of the clean sources of energy which has expanded rapidly in recent years is the offshore wind energy. With the growing interest in deployment of new offshore wind farms in Europe and worldwide, it is important to improve the best practice in structural integrity assessment of the offshore wind turbines. Similar to other offshore structures such as Oil & Gas pipelines, the offshore wind turbines are subjected to cyclic loading conditions during the

* Corresponding author.
E-mail address: a.mehmanparast@cranfield.ac.uk

2452-3216
Peer-review under responsibility of the ECF22 organizers.
10.1016/j.prostr.2018.12.044

operation due to wind, wave and current loads causing fatigue damage in these fleets. In addition to fatigue damage, corrosion damage plays a significant role in material degradation, pitting and crack initiation ad propagation in offshore wind turbine structures, particularly in the foundations which are in direct contact with seawater. Therefore, in order to accurately estimate the lifetime of the offshore wind turbine foundations, corrosion-fatigue crack growth tests need to be performed on fracture mechanics specimens geometries to characterize the crack propagation behavour of the material. Corrosion-fatigue tests are known to be considerably time consuming and costly, due to low testing frequencies which may result in several months of testing on each sample. Moreover, given that the test must be repeated for different load levels in order to obtain an understanding of material behaviour in a wide range of realistic loading conditions, the required time for testing increases drastically.

In order to characterize the crack propagation behavior in offshore wind turbine foundations for free-corrosion conditions, corrosion-fatigue tests are often performed on compact tension, C(T), fracture mechanics specimens [1]. Once a C(T) specimen is manufactured, it is soaked in seawater and fatigue cyclic are applied to the specimen. An important challenge in corrosion-fatigue testing is crack growth monitoring on specimen soaked in seawater. In this paper, a numerical finite element analysis model has been developed to estimate the crack length in C(T) specimens using the back face strain (BFS) measurement technique. The numerical predictions are presented in this paper and the results are validated through comparison with experimental data.

Nomenclature

a	Crack length
B	Specimen thickness
E	Elastic Young's modulus
H	Specimen half height
L	Specimen half thickness
P_{max}	Maximum load level in fatigue cycle
R	Load ratio
W	Specimen width
v	Poisson's ratio
BFS	Back face strain measurement

2. Development of a finite element model t predict back face strain variations

2.1. Development of experimental calibration curves

In order to estimate the instantaneous crack length, a, in corrosion-fatigue tests, calibration tests are firstly performed in air to generate an empirical crack length vs. BFS correlation curve (see Figure 1). The basis of the BFS technique is that as the crack propagates the bending strain at the back of the sample increases. Therefore, by attaching a strain gauge at the back of the sample, an experimental correlation between the crack length and the BFS can be developed for a given loading condition.

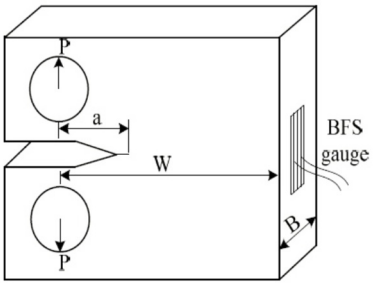

Figure 1: Schematic demonstration of BFS measurement at the back of the sample

These calibration curves are sensitive to the applied load level, hence with a change in the loading condition in a corrosion-fatigue test a new calibration test needs to be performed to find a new load-specific empirical correlation between a and BFS.

2.2. Finite element modelling of back face strain variation

A 3D finite element model was developed in ABAQUS to predict the BFS variation in a C(T) specimen geometry with the width of W = 50 mm and the thickness of B = 16 mm. As seen in Figure 2, an appropriate petitioning strategy was adopted to assign fine elements along the crack path and also at the back of the sample where the BFS values are predicted. There were approximately 800,000 elements in the model with the smallest element size of 100 μm located along the crack path and at the back face of the C(T) geometry. It's worth noting that 100 μm was found as the optimum element size in the model after performing a mesh sensitivity analysis.

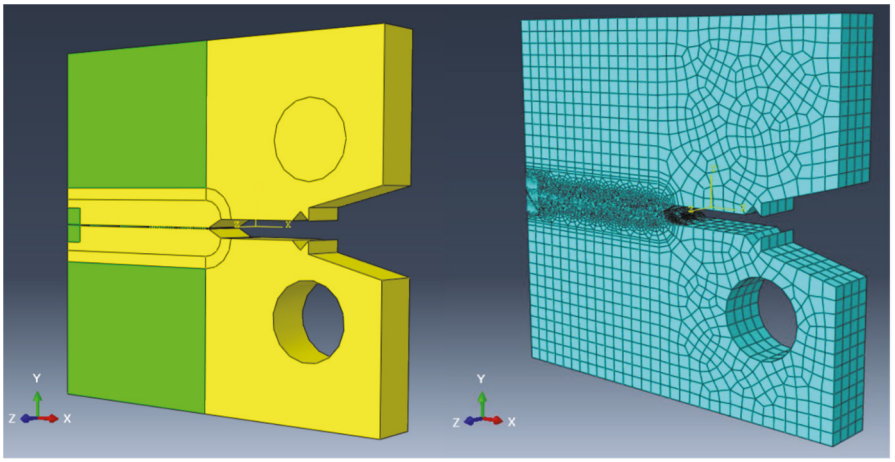

Figure 2: (a) Partitioned C(T) geometry in ABAQUS (b) the mesh structure of the C(T) specimen

2.3. Combined isotropic-kinetic hardening model

The material of interest in this study is S355 structural steel which is widely used in offshore applications. As shown in [2] the elastic properties of S355 are E = 190 GPa and Poisson's ratio of v = 0.3. In order to capture the Bauschinger effect in the hardening behavior of the material, cyclic tests need to be performed across different strain ranges. In the cyclic tests, if the yield stress in repeat cycles increases the material is subject to hardening and if it decreases the material shows a softening behavior. Several studies have been conducted to investigate the hardening behaviour of S355 steel and they revealed an interesting behaviour in this material. It was observed by Mrozinski and Piotrowski [3] that at high strain levels the material shows a hardening behavior whereas at low strain cycles of less than 0.5% the material exhibits a softening behavior. This has also been confirmed from the experiments completed by Jesus et al [2], which were conducted for a comparison between S355 and S690 cyclic behaviour. To accurately describe the hardening behaviour of the material, the combined isotropic-kinematic model was used, which is also recommended from ABAQUS documentation as the most accurate model for materials subjected to cyclic loading [4]. The general equation that describes the hardening law is:

$$\dot{\alpha_k} = C_k \frac{1}{\sigma^0}(\sigma - \alpha)\dot{\bar{\varepsilon}}^{pl} - \gamma_k \alpha_k \dot{\bar{\varepsilon}}^{pl} \quad (1)$$

where the overall backstress is calculated as:

$$\alpha = \sum_{k=1}^{N} \alpha_k \quad (2)$$

and σ^0 is the yield surface size, N is the number of back stresses, C_k and γ_k are material parameters that need to be calibrated using cyclic test data. C_k is defined as the initial kinematic hardening modulus, while γ_k determines the rate at which this modulus decreases/increases as plastic strain increases.

The isotropic hardening component defines the evolution of the yield surface size, σ^0, as a function of equivalent plastic strain, $\bar{\varepsilon}$, using an exponential equation:

$$\sigma^0 = \sigma|_0 + Q_\infty(1 - e^{-b\bar{\varepsilon}^{pl}}) \quad (3)$$

where $\sigma|_0$ is the yield stress at zero plastc strain, and Q_∞ and b are material constants that define the maximum change in the size of the yield surface and the rate at which the size of the yield surface changes as plastic strain increases, respectively [5].

In this work $\sigma|_0$ is taken as the yield stress of the material which is 400 MPa accordingly to ref [2]. C and γ values are identified using the stabilized hysteresis loops which correspond to different strain amplitudes of 0.3%, 0.5%, 0.8%, 1% and 1.2% taken from ref [3]. The values for these two parameters were found as C = 387 MPa and γ=1.8 by doing iteration in Matlab. Alternatively, the isotropic hardening parameters were found as Q_∞=340 MPa and b = 45.

3. Back face strain prediction results

Simulations were performed by applying a sinusoidal cyclic loading condition on the C(T) specimen using the load ratio of R = 0.1 and maximum load of P_{max} = 7, 8, 12 and 14 kN. For each load case, simulations were performed at different crack lengths ranging from 20 mm to 30 mm which correspond to $0.4 < a/W < 0.6$. The BFS in each simulation has been analyzed by taking the average strain within the strain gauge measurement area to replicate the BFS measurements from experiments as schematically shown in Figure 3(a). The strain gauge coverage area at the back face of the sample is 6 mm in Y direction and 3 mm in Z direction for the tests performed in this study. An example of the back face strain variation along Y-axis and Z-axis at different crack lengths for P_{max} = 8 kN is shown in Figure 3(b) and Figure 3(c), respectively. Note that the strain variation in these two figures have been presented in normalized form, with respect to the specimen half height, H, and half thickness, L. As seen in these figures, the local strain variation strongly depends on the Y-coordinate while negligible variations are observed along through thickness axis, Z. Therefore, for area averaged BFS analysis, only the strain values along the Y-axis, which show a much more prominent effects on strain values, have been considered. Also seen in Figure 3(b) and Figure 3(c) is that the BFS values are strongly sensitive to the crack length and as the normalized crack length, a/W, increases the magnitude of BFS significantly increases along both Y and Z axes.

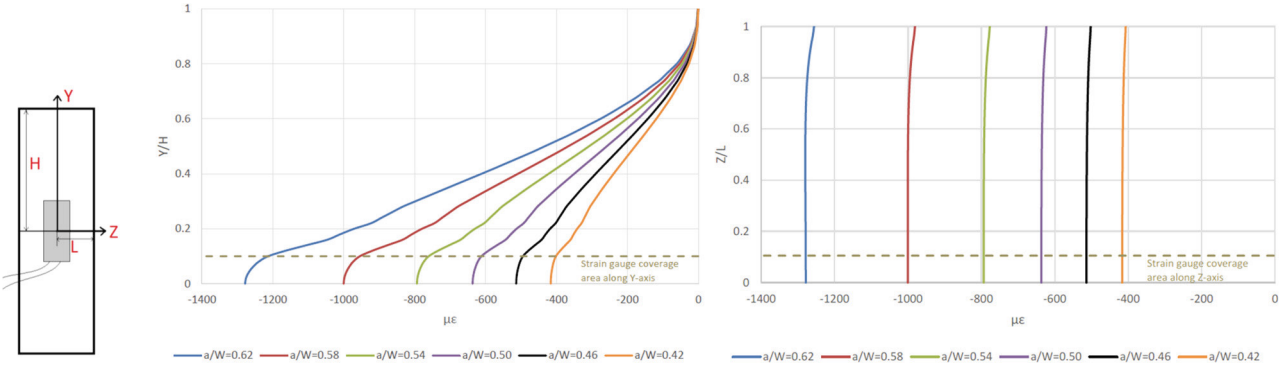

Figure 3: (a) BFS measurement area in the experiment and FE simulation (b) an example of strain variation along Y-axis at different crack lengths (c) strain variation along Z-axis at different crack lengths

The crack length values are plotted against averaged values of back face strain predictions for different load levels in Figure 4. Also included in this figure are the experimental a vs. BFS calibration curves for P_{max} values of 1.5, 4, 6, 7, 8, 10 and 12 kN which have been obtained from tests on C(T) specimens with identical dimensions (i.e. W= 50 mm and B =16 mm) [1]. As seen in this figure, the predicted results follow the same trend as the experimental curves. However, for a given value of BFS, the crack lengths obtained from FE simulations are slightly overestimated compared to the experimental curves which can be due to the yield stress and material properties variation in different subgrades of S355 steel. The obtained results from FE simulations provide a very good approximation of the crack length with 0.5-0.7 mm difference with the experimental data throughout the range of a/W and P_{max} examined in this work. This corresponds to maximum 6% error in crack length estimation from the developed finite element model. It must be noted that the experimental a vs. BFS calibration curves are based on the crack length measurements using the optical technique at the outer surface of the sample. The instantaneous crack lengths are often monitored on both faces and averaged to generate a calibration curve. However, the outer surface measurement does not account for possible crack tunneling throughout the specimen thickness in fatigue and corrosion-fatigue crack growth tests. Therefore, some inaccuracies might be involved in experimental a vs. BFS calibration curves.

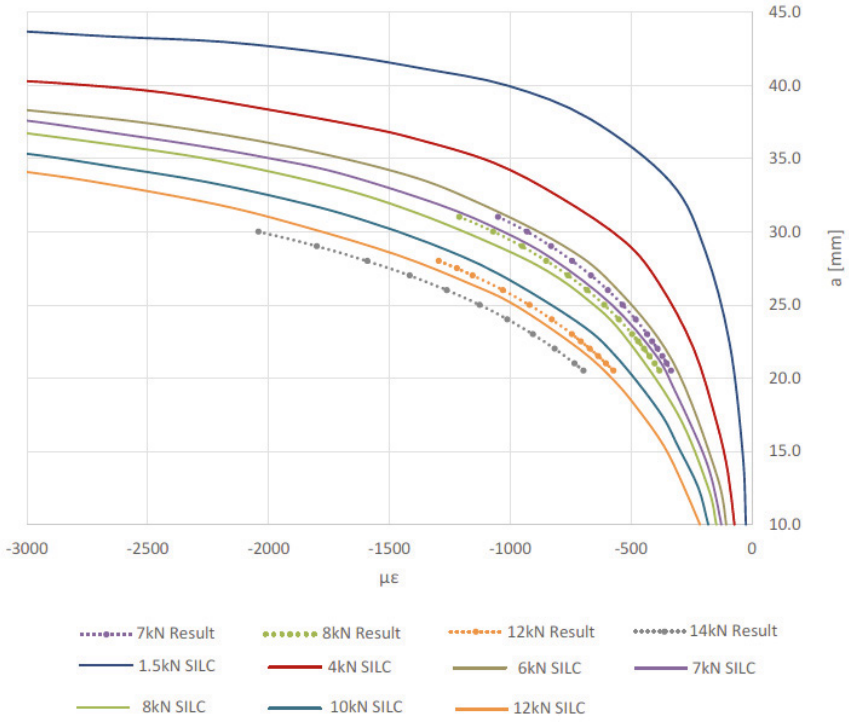

Figure 4: Comparison of a vs. BFS predictions with experimental curves

In order make the analysis easier for crack length estimation at a given BFS value based on the numerical results, a polynomial equation has been derived to express the variation in calibration curves for different crack lengths and load levels which is described as:

$$\frac{a}{W} = A_0 + A_1\varepsilon + A_2\varepsilon^2 + A_3\varepsilon^3 \quad (4)$$

where ε is the average BFS value, and A_0, A_1, A_2 and A_3 are load dependent parametric coefficients. Note that for different load levels examined in this work the R^2 value was greater than 0.98 indicating an accurate fit made to the numerical data using the proposed equation. The values of parametric equations for different load levels are summarized in Table 1.

Table 1: Values of the load dependent parametric coefficients

P_{max} (kN)	A_0	A_1	A_2	A_3
7	1.60×10^{-1}	-9.96×10^{-4}	-8.00×10^{-7}	-2.00×10^{-10}
8	1.60×10^{-1}	-8.64×10^{-4}	-6.00×10^{-7}	-1.80×10^{-10}
12	1.29×10^{-1}	-6.84×10^{-4}	-4.00×10^{-7}	-1.00×10^{-10}
14	1.54×10^{-1}	-4.94×10^{-4}	-2.00×10^{-7}	-4.00×10^{-11}

4. Conclusions

Finite element simulations have been performed on C(T) specimen geometry with the width of W = 50 mm and thickness of B = 16 mm to predict the correlation between crack length and back face strain measurements for S355 structural steel. The numerical calibration curves have been developed for a range of load levels, and the results are compared with the experimental data. Moreover, based on the numerical results a general equation has been proposed to describe the variation in BFS as a function of crack length for various load levels. A combined isotropic-kinematic hardening model was used in the analysis with the hardening parameters identified using the cyclic data available in the literature on S355 steel. The results have shown that the predicted a vs. BFS curves from finite element simulations follow the same trend as the experimental data. Also for the range of load levels examined and for a given values of BFS, the estimated crack length has a good agreement with the experimental data with maximum 6% error in crack length estimations. Considering the experimental errors which might be encountered in experimental crack growth monitoring, due to crack length measurements at the outer surface which do not account for through thickness crack tunneling, the developed finite element model provides an acceptable estimate of crack length calculated using the proposed equation for a given value of BFS.

References

[1] Mehmanparast A, Brennan F, Tavares I. Fatigue crack growth rates for offshore wind monopile weldments in air and seawater: SLIC inter-laboratory test results. Materials & Design. 2017;114:494-504.
[2] de Jesus AMP, Matos R, Fontoura BFC, Rebelo C, Simões da Silva L, Veljkovic M. A comparison of the fatigue behavior between S355 and S690 steel grades. Journal of Constructional Steel Research. 2012;79:140-50.
[3] Mrozinski S, Piotrowski M. Effect of strain level on cyclic properties of S355 steel. AIP Conference Proceedings: AIP Publishing; 2016. p. 020005.
[4] ABAQUS. User Manual. in Version 6.14 ed: in Version 6.14, SIMULIA; 2016.
[5] Lemaitre J, Chaboche J-L. Mechanics of solid materials: Cambridge university press; 1994.